**Naval Research Laboratory**
**Stennis Space Center, MS 39529-5004**

**NRL/MR/7176--98-8080**

# Internal Waves in the SESAME II Experiment: Speed, Direction, and Effect on Acoustic Transmission

JACOB GEORGE
ROBERT L. FIELD

*Ocean Acoustics Branch*
*Acoustics Division*



April 2, 1998

# REPORT DOCUMENTATION PAGE

*Form Approved*
*OBM No. 0704-0188*



| 1. AGENCY USE ONLY *(Leave blank)* | 2. REPORT DATE | 3. REPORT TYPE AND DATES COVERED |
|---|---|---|
| | April 2, 1998 | Final |

**4. TITLE AND SUBTITLE**

Internal Waves in the SESAME II Experiment: Speed, Direction, and Effect on Acoustic Transmission

**5. FUNDING NUMBERS**

*Job Order No.* 571668008
*Program Element No.* 0602435N
*Project No.*
*Task No.* 03591
*Accession No.*

**6. AUTHOR(S)**

Jacob George and Robert L. Field

**7. PERFORMING ORGANIZATION NAME(S) AND ADDRESS(ES)**

Naval Research Laboratory
Acoustics Division
Stennis Space Center, MS 39529-5004

**8. PERFORMING ORGANIZATION REPORT NUMBER**

NRL/MR/7176--98-8080

**9. SPONSORING/MONITORING AGENCY NAME(S) AND ADDRESS(ES)**

Office of Naval Research
800 N. Quincy Street
Arlington, VA 22217-5000

**10. SPONSORING/MONITORING AGENCY REPORT NUMBER**

**11. SUPPLEMENTARY NOTES**

**12a. DISTRIBUTION/AVAILABILITY STATEMENT**

Approved for public release; distribution unlimited

**12b. DISTRIBUTION CODE**

**13. ABSTRACT** *(Maximum 200 words)*

The SESAME II experiment was conducted off the northwestern coast of Scotland in July/August 1996. Three vertical arrays (named "the deep array," the shallow array," and "the temperature array") containing thermal sensors and hydrophones were deployed. An analysis of temperature and sound speed data from the experiment over a 5-day span reveals that the relatively long period variations can be identified with the M2 tidal cycles (principal lunar tides with period 12.42 h). Short period events (of about 10 min duration) on the shallow array are usually accompanied by similar, though not identical, events on the temperature array, delayed by 2–10 min. Such correspondence was found to be rare between the deep array and the shallow array. The time delays correspond to a range of internal wave (IW) speeds of 0.15–0.35 m/s. During the 5-day period, a search for prominent short-period events (soliton-like events) in which the isospeed contour dips from a depth of about 50 m to a depth of over 120 m on both arrays, reveals several candidates at days 215.35, 217.6, 218.65, 218.97, 219.48, 219.6, and 219.74. Among these, the event at day 217.6 seems closest to being soliton-like because it retained its shape more perfectly than others while traveling from the shallow array to the temperature array. Assuming its direction (the wave-vector direction) to be approximately toward southeast with compass angle 105° (the average value obtained from analysis of current-meter data), its speed would be 0.3 m/s, in excellent agreement with the value of 0.35 m/s, also obtained from current-meter data. During the middle period of this soliton-like event, the sound speed profile has been found to possess approximately constant gradient. According to a well-known theorem, such a constant gradient sound speed profile should cause refraction of the sound energy passing through the IW.

**14. SUBJECT TERMS**

shallow water, internal waves, solitons, sound propagation

**15. NUMBER OF PAGES**

30

**16. PRICE CODE**

| 17. SECURITY CLASSIFICATION OF REPORT | 18. SECURITY CLASSIFICATION OF THIS PAGE | 19. SECURITY CLASSIFICATION OF ABSTRACT | 20. LIMITATION OF ABSTRACT |
|---|---|---|---|
| Unclassified | Unclassified | Unclassified | SAR |

## 1. INTRODUCTION

The purpose of the present report is to document some results obtained in analyzing data from the SESAME II experiment. The SESAME II experiment was conducted off the north-western coast of Scotland in July/August 1996. Two of the goals of this experiment were to measure the internal wave (IW) activity in this region and to determine their effect on acoustic transmission[1].

Data over a 5 day period, including a time of acoustic transmission, were analyzed. Temperature and sound speed variations of relatively long durations (about 12 hrs), and those of relatively short durations (about 10 mins), are discussed below. The direction and speed of an observed soliton-like event, as well as those of other IWs, are analyzed. Their effect on acoustic transmission is discussed.

## 2. EXPERIMENT OVERVIEW

The experimental geometry of SESAME II is shown in Fig. 1. The "shallow array" was a vertical array of thermal sensors and hydrophones, deployed in 170 m of water. The "deep array" was a similar array deployed in 500 m of water. The "temperature array" contained only thermal sensors. Thermal sensors on the shallow array and the deep array were at depths 25, 30, 35, 40, 45, 50, 55, 65.5, and 150 m. The temperature array had thermal sensors at the above depths, and at a depth of 11 m.

Temperature samples were recorded at time intervals of 0.0014 days (2.016 min). The corresponding sound speeds were calculated from the temperature samples and salinity, which was practically constant. Since the effect of IWs on sound propagation is of prime interest, the analysis below has been done using the above sound speed values.

## 3. EFFECT OF TIDAL CYCLES ON SOUND SPEED

Sound speed variations calculated from temperature data recorded by the sensor at depth 55 m are shown in Fig. 2(a) for the shallow array, and Fig. 2(b) for the temperature array. The time series from the sensor at depth 55 m is presented because that time series contains both variations of relatively long durations (about 12 hrs), and those of relatively short durations (about 10 mins); but with not too many short period events to cause confusion. Data over the 5 day period (days 215 - 220) has been the subject of the present analysis.

The influence of tidal cycles on the data can be demonstrated by calculating moving averages

of the curves in Figs. 2 (a) and (b). The result of calculating averages over a moving window of length 141 samples (time span of 0.1974 days = 4.7376 hrs) is shown in Fig. 3 (solid line: shallow array, dashed line: temperature array). The peaks from the shallow array and the temperature array occur at the same times. There are 9 peaks plus a sizable fraction of a $10^{th}$ peak over 5 days, in excellent agreement with the 9.7 peaks expected from an M2 cycle (principal lunar tide with period 12.42 hrs). Thus, the M2 tidal cycle accounts for most of the long period variations.

Sound speed variations averaged over a moving window of length 141 samples (time span of 0.1974 days = 4.7376 hrs) from all the sensors are shown in Fig. 4(a) for the shallow array, and Fig. 4(b) for the temperature array. In Figs. 4 (a) and (b), a lower curve corresponds to a deeper sensor. This is understandable, since in the present case the sound speed generally decreases with depth. The relatively small temperature variations at depths 11 m and 150 m account for the relatively flat curve that lies highest in Fig. 4(b), and the two relatively flat curves that lie lowest in Figs. 4 (a) and (b).

## 4. SHORT PERIOD VARIATIONS

Isospeed contours of 1494.5 m/s, as functions of depth and time, are shown in Figs. 5(a)-(j) (solid line: shallow array, dashed line: temperature array). The value of 1494.5 m/s was chosen because, for that value, the contour spans most of the water column from top to bottom. Short period events of about 10 min duration on the shallow array (solid line) are usually accompanied by similar, though not identical, events on the temperature array (dashed line), delayed by 2 - 10 min. Such correspondence was found to be rare between the deep array and the shallow array; therefore the present analysis has been done using only the shallow array and the temperature array.

For an IW plane wave travelling approximately towards the south-east direction, the time delay $t_{ST}$ between the wavefront crossing the shallow array and the temperature array can be expressed in terms of the IW speed v, the ranges, and the angles (Fig. 1) as

$$t_{ST} = \frac{R_2 \sin\left(90^o - \theta - \phi_2\right)}{v} . \qquad (1)$$

Assuming the IW incident angle to be $\theta = 15^o$ (the average value obtained from current meter analysis[2]), Eq. (1) can be used to calculate the IW speeds corresponding to the time delays $t_{ST}$ of prominent short period events. These are shown in Fig. 6.

## 5. IDENTIFICATION OF SOLITON-LIKE EVENTS

In the present analysis, a soliton is taken to be "a wave of permanent form"[3]. The IW wave-vectors here usually point approximately towards the south-east direction, and are incident nearly perpendicularly to the line joining the shallow array and the temperature array. Therefore, in addition to solitons, even a linear dispersive wave propagating in that direction may look very similar on the two arrays, which were separated by a range of only 433 m. Thus, it is appropriate to search for events which resemble solitons (soliton-like events), though they really may not be solitons. A search of Figs. 5(a)-(j) for such events, especially prominent short-period events in which the isospeed contour dips from a depth of about 50 m to a depth of over 120 m on both arrays, reveal several candidates at days 215.35, 217.6, 218.65, 218.97, 219.48, 219.6, and 219.74. Among these, the event at day 217.6 seems closest to being soliton-like, because it retained its shape more perfectly than others while traveling from the shallow array to the temperature array. This is demonstrated in Fig. 7, where the isospeed contour for the shallow array (solid curve) has been shifted by 4 sampling intervals (0.0056 days = 8.064 min.) to the right to make the event at day 217.6 on the shallow array and the temperature array coincide.

## 6. CONTSTRAINTS ON SPEED AND DIRECTION OF SOLITON-LIKE EVENT

For the soliton-like event at day 217.6, the travel time from the shallow array to the temperature array is 0.0056 days (8.064 min.). Given this travel time, Eq. (1) constrains the possible values of the event's speed and direction. That relationship is shown in Fig. 8. For a direction given by $\theta = 15^{\circ}$ (the average value obtained from analysis of current meter data[2]), the speed of the soliton-like event from this graph would be 0.3 m/s, in excellent agreement with the value of 0.35 m/s also obtained from current meter data[2].

## 7. EFFECT ON SOUND SPEED PROFILE AND TRANSMISSION

The evolution of sound speed profiles during the period that includes the soliton-like event at day 217.6 is shown in Fig. 9(a). For clarity of presentation, the profiles from successive samples (sampling interval: 0.0014 days = 2.016 min) have been incremented by 5 m/s. In Fig. 9(a), the profiles at the beginning and at the end are isospeed over depths of 50 m to 150 m, with a steady increase in sound speed from the depth 50 m to the ocean surface. But profiles during the middle period have a clearly different appearance, and are closer to straight lines. Even though the appearance of the strictly linear profile between the depths of 65.5 and 150 m is the result of interpolation (because there are no sensors between the depths of 65.5 and 150 m), nevertheless the profiles in the middle period can be approximately characterized as possessing a constant gradient. Similar sound speed profile histories corresponding to the soliton-like events at days 218.65 and

219.48 are shown in Figs. 9(b) and 9(c), respectively.

It is well known that in such a constant sound speed gradient region, the acoustic ray path would be an arc of a circle of radius[4]

$$R = c_0 / g, \tag{2}$$

where $c_0$ is the average sound speed, and g is the magnitude of the sound speed gradient with respect to depth. From Fig. 9(a), the gradient is 0.092 (m/s)/m, and the radius is 16.3 km. The effect of such a gradient is illustrated with an example in Fig. 10, where the ranges 0 - 400 m and 1600 - 2000 m are isospeed regions. The range 400 - 1600 m has the constant gradient profile from the middle period of Fig. 9(a), such that the radius of the circular ray arc is 16.3 km. The paths of several rays in such an environment are shown. The main effect of the constant gradient region is to cause refraction.

## 8. SOLITON-LIKE EVENTS DURING ACOUSTIC TRANSMISSION

Isospeed contours of 1494.5 m/s as functions of depth and time during the acoustic transmission experiment, are shown in Fig. 5(j). (Solid line: shallow array, dashed line: temperature array). During the time of the experiment, there is one prominent short-period event in which the isospeed contour dips from a depth of about 50 m to a depth of over 120 m on both arrays. That event occurs at day 219.74.

## 9. CONCLUSIONS

The above analysis of temperature and sound speed data from SESAME II over a 5 day span reveals that the relatively long period variations can be identified with the M2 tidal cycles (principal lunar tides with period 12.42 hrs). Short period events (of about 10 min duration) on the shallow array are usually accompanied by similar, though not identical, events on the temperature array, delayed by 2 - 10 min. Such correspondence was found to be rare between the deep array and the shallow array. The time delays correspond to a range of IW speeds of 0.15 - 0.35 m/s. During the 5 day period, a search for prominent short-period events (soliton-like events) in which the isospeed contour dips from a depth of about 50 m to a depth of over 120 m on both arrays, reveal several candidates: at days 215.35, 217.6, 218.65, 218.97, 219.48, 219.6, and 219.74. Among these, the event at day 217.6 seems closest to being soliton-like, because it retained its shape more perfectly than others while traveling from the shallow array to the temperature array. Assuming its direction (the wave-vector direction) to be approximately towards south-east, with compass angle 105$^{\circ}$ (the average value obtained from analysis of current-meter data[2]), its speed would be 0.3 m/s, in

excellent agreement with the value of 0.35 m/s, also obtained from current-meter data[2]. During the middle period of this soliton-like event, the sound speed profile has been found to possess approximately constant gradient. According to a well known theorem, such a constant gradient sound speed profile should cause refraction of the sound energy passing through the IW[4].

## 10. ACKNOWLEDGMENTS

It is a pleasure to thank Dr. Zachariah R. Hallock for several enlightening discussions. This work was supported by the Office of Naval Research and the Naval Research Laboratory.

## REFERENCES

1. R. L. Field, C. Mire, Z. R. Hallock, J. George, and M. K. Broadhead, "The SESAME experiments - The effects of internal solitons on acoustic propagation on the Malin shelf", International Conference on Shallow Water Acoustics, Beijing, China (1997) (to be published).

2. Z. R. Hallock, J George, J. Small, and R. L. Field, "Upslope internal wave propagation on the Malin shelf", (in preparation)

3 P. G. Drazin and R. S. Johnson, *Solitons: An Introduction*, Cambridge U. (1993), Section 1.3, p.15.

4. R. J. Urick, *Principles of Underwater Sound*, McGraw-Hill, New York (1983), p. 125.

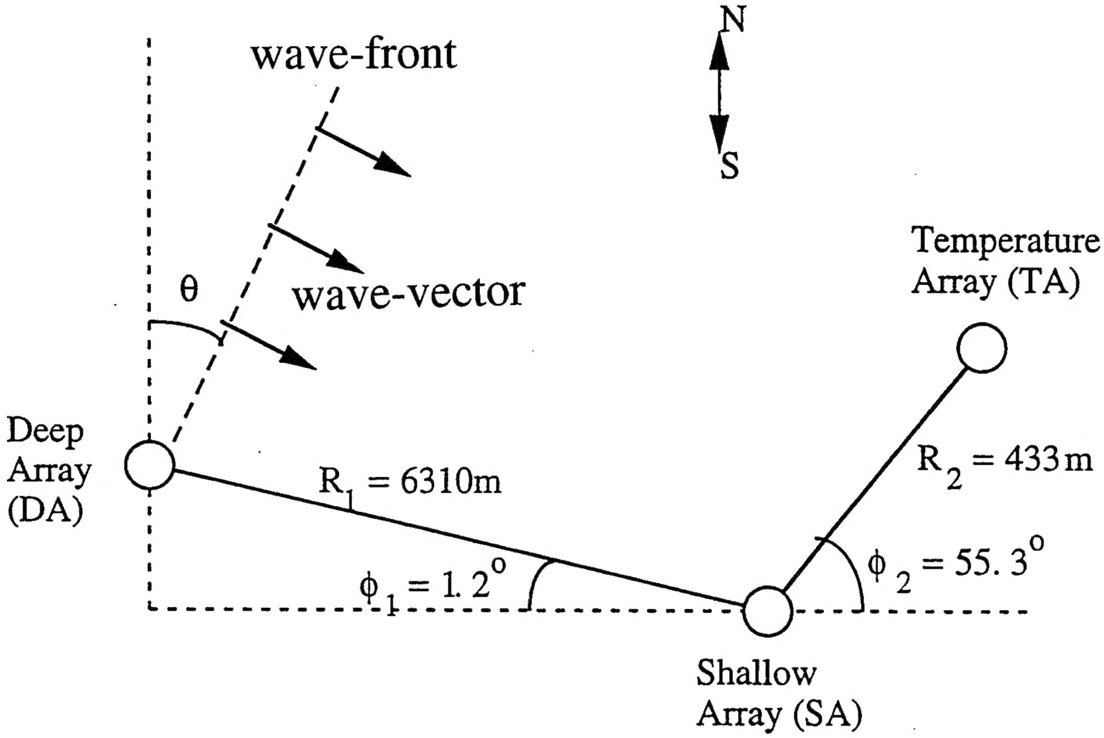


Figure 1. SESAME II experimental geometry, showing array positions and IW direction.

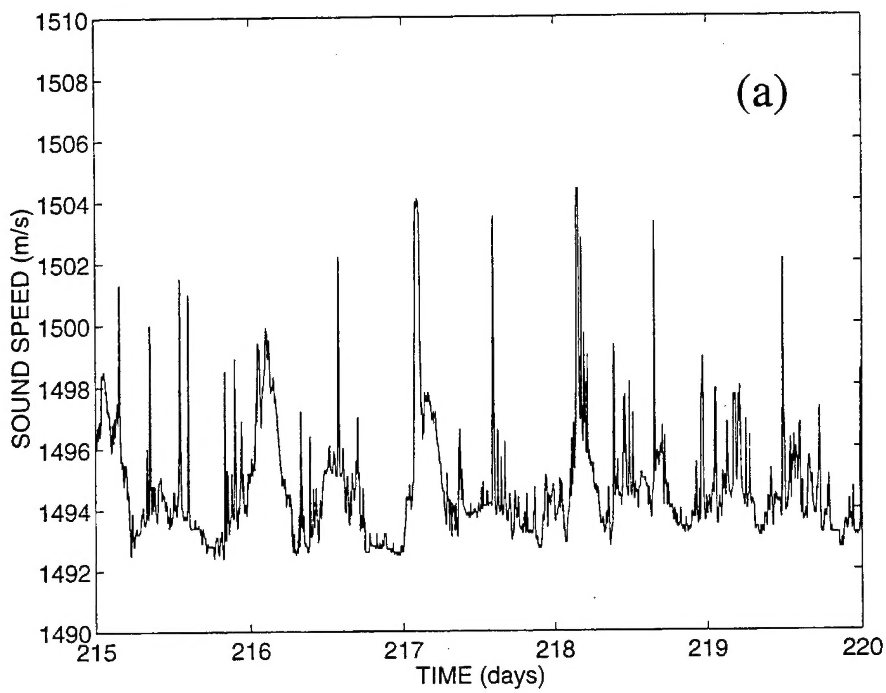


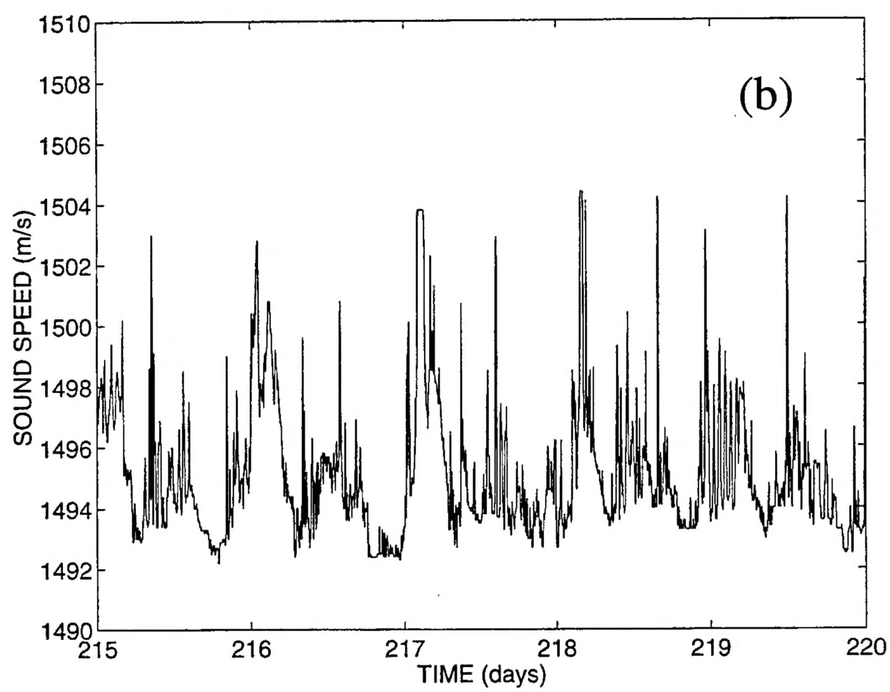


Figure 2. Sound speed variations calculated from temperature data recorded by the sensor at depth 55 m. (a) shallow array, (b) temperature array.

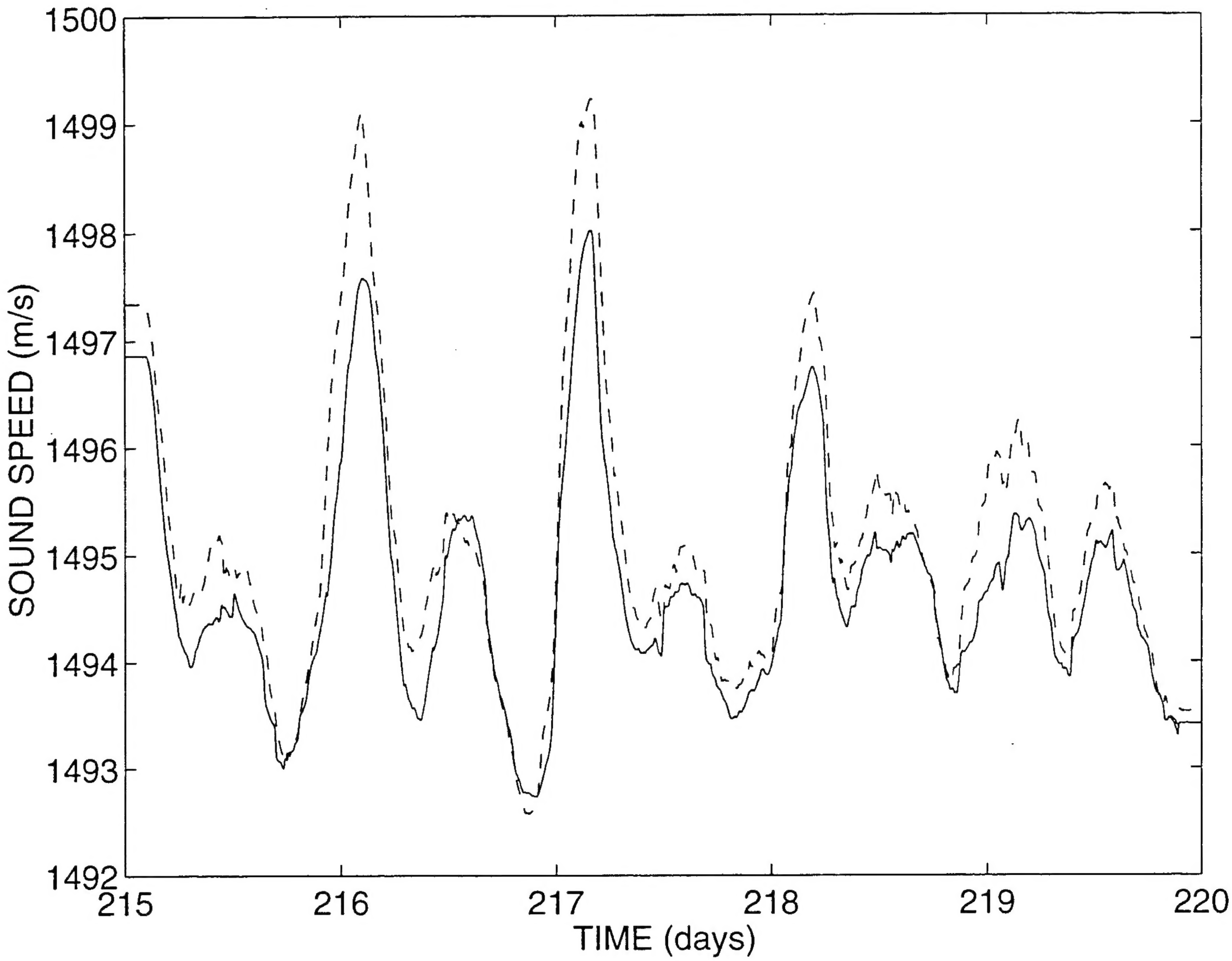


Figure 3. Sound speed variations averaged over a moving window of length 141 samples (time span of 0.1974 days = 4.7376 hrs), from the sensor at depth 55 m. Solid line: shallow array, dashed line: temperature array.

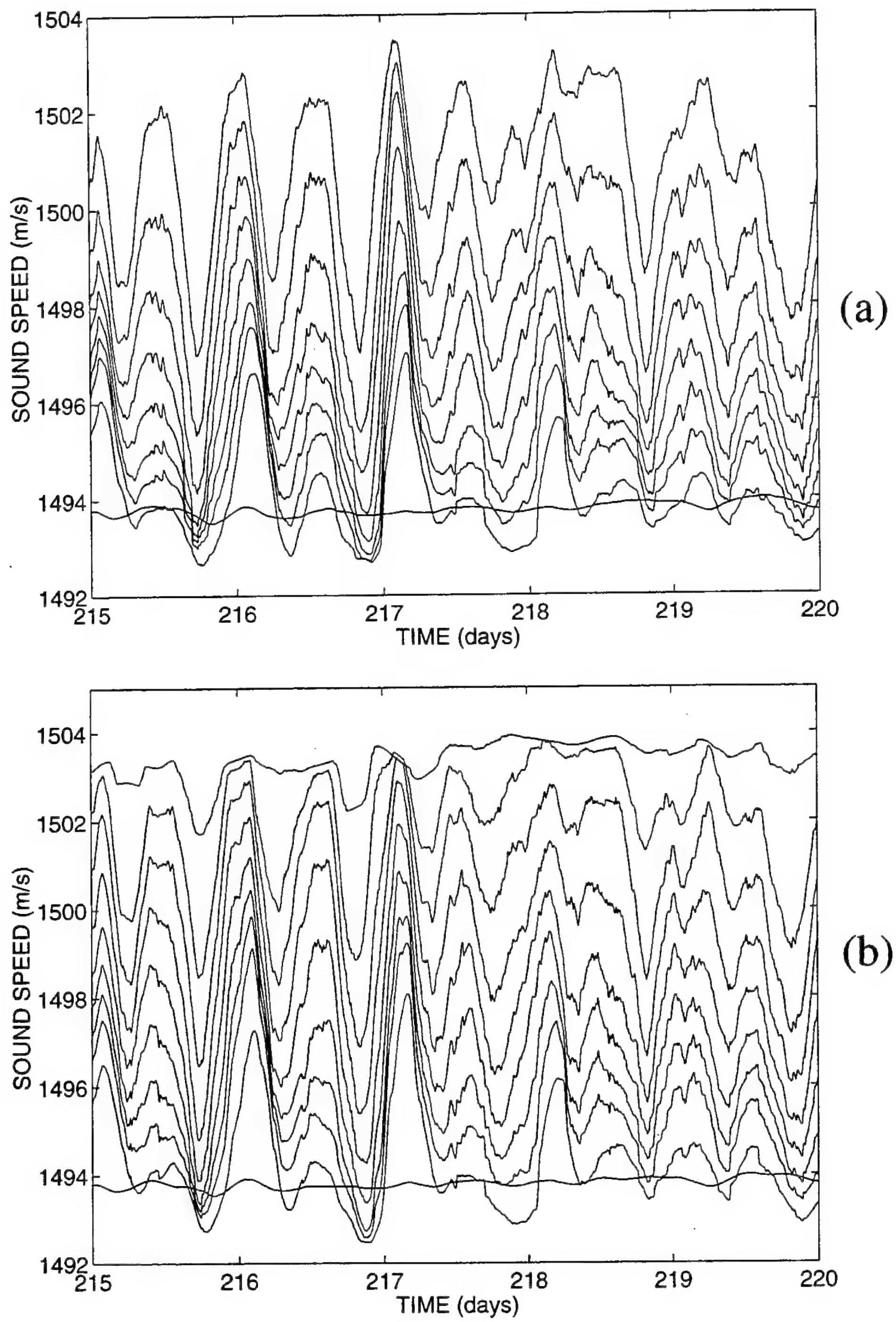


Figure 4. Sound speed variations averaged over a moving window of length 141 samples (time span of 0.1974 days = 4.7376 hrs), from sensors at depths 25, 30, 35, 40, 45, 50, 55, 65.5, and 150 m, from (a) shallow array, and (b) temperature array. The temperature array contains an additional sensor at 11 m. In (a) and (b), a lower curve corresponds to a deeper sensor.

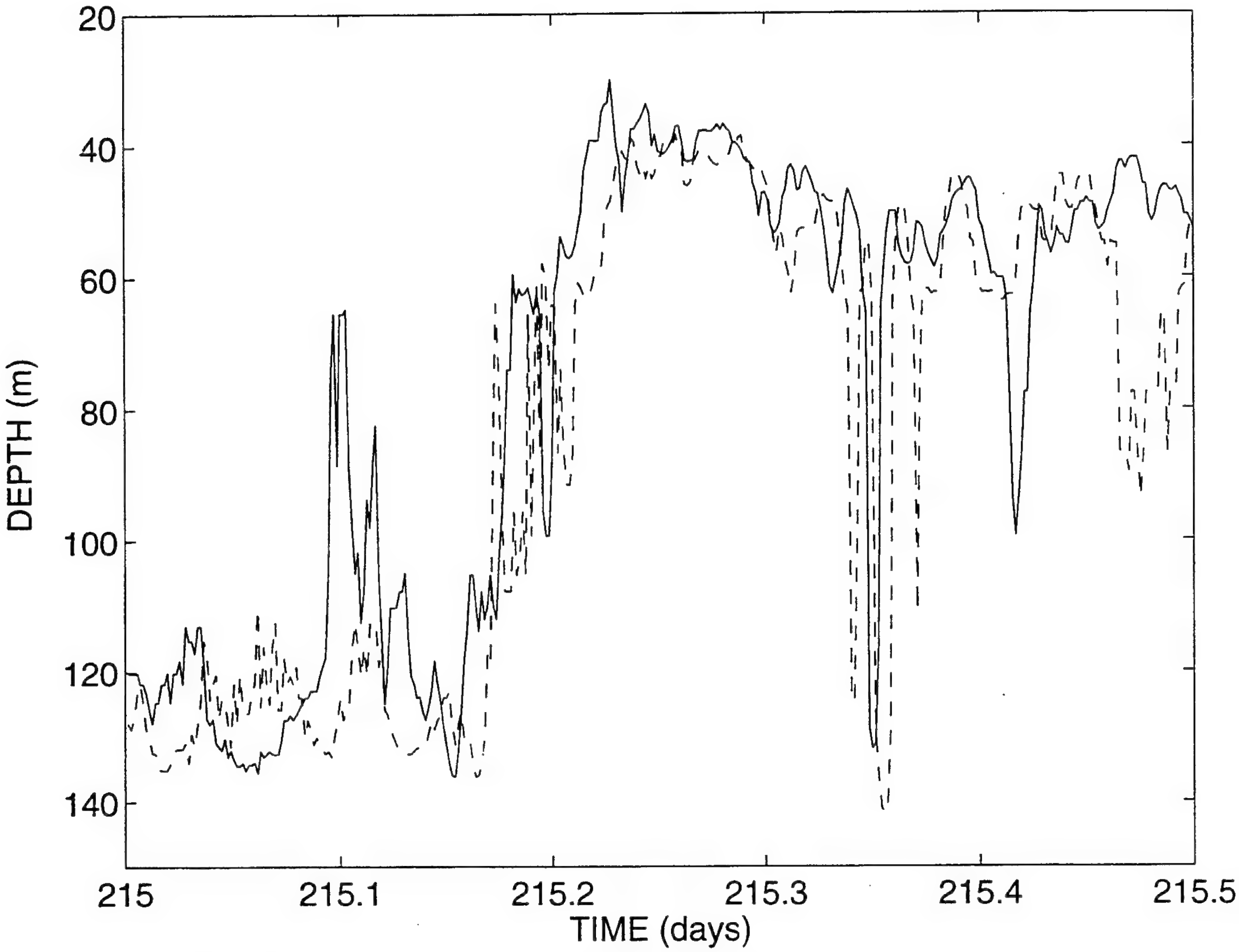


Figure 5(a). Isospeed contours of 1494.5 m/s as functions of depth and time. Solid line: shallow array, dashed line: temperature array. Days 215.0 - 215.5.

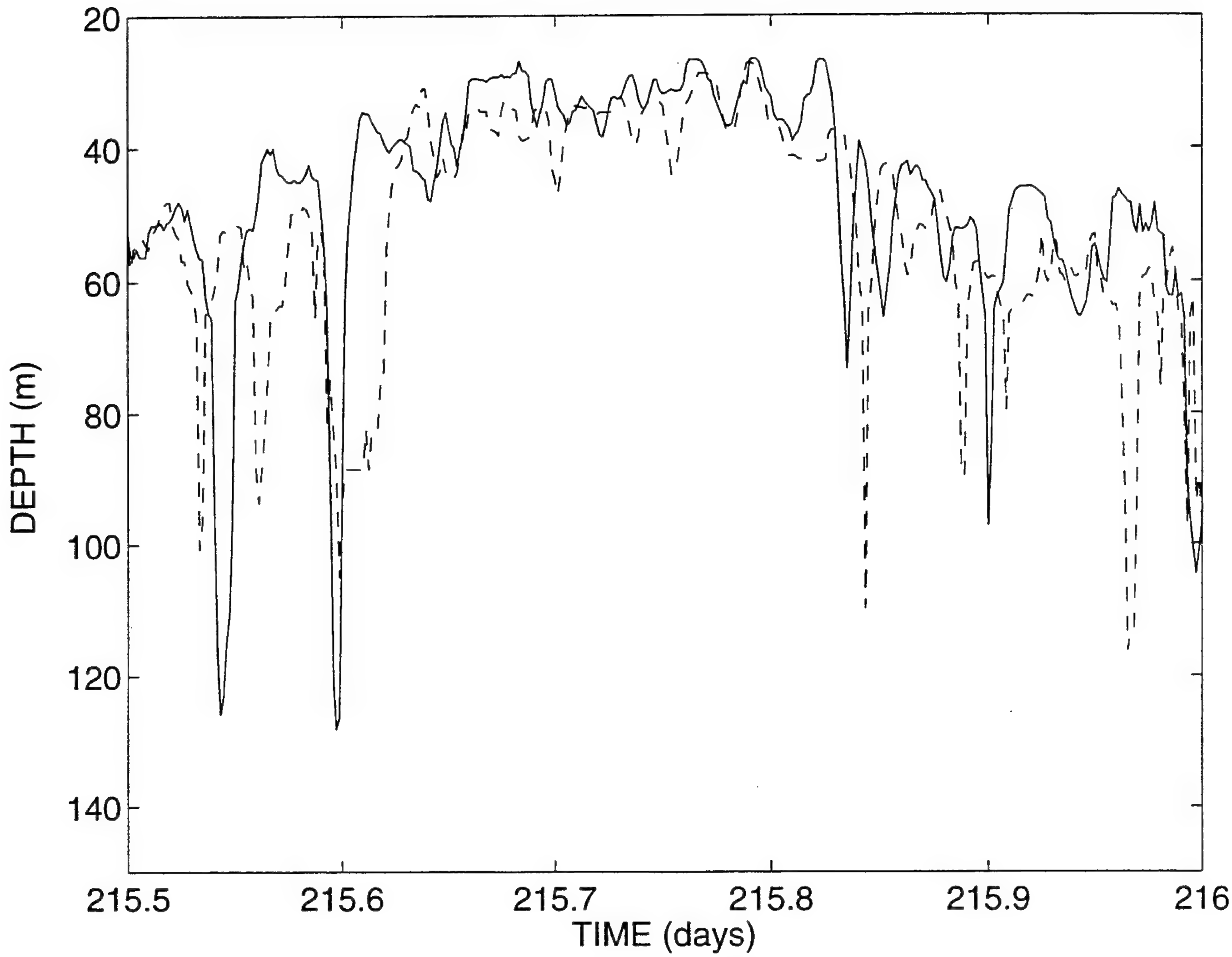


Figure 5(b). Isospeed contours of 1494.5 m/s as functions of depth and time. Solid line: shallow array, dashed line: temperature array. Days 215.5 - 216.0.

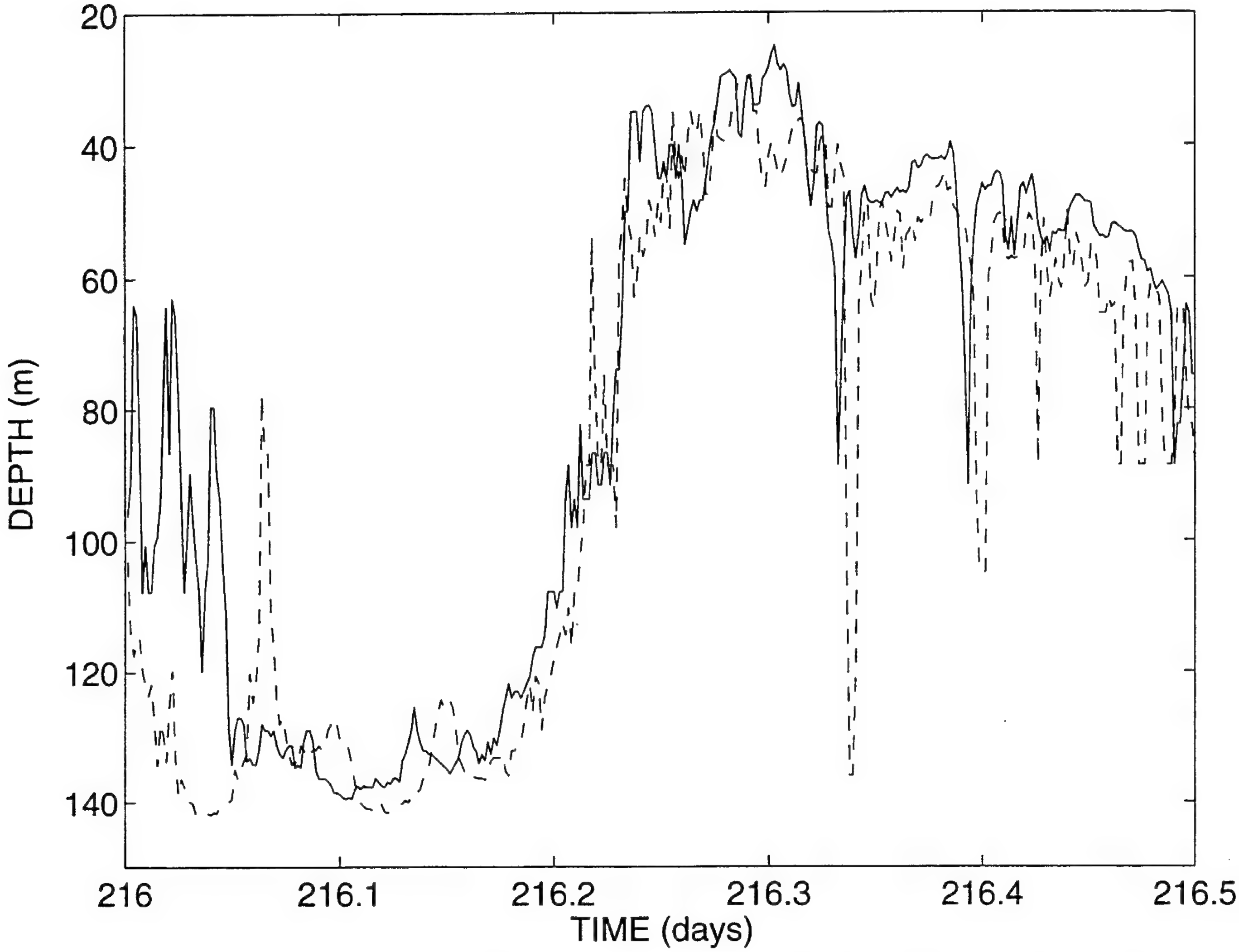


Figure 5(c). Isospeed contours of 1494.5 m/s as functions of depth and time. Solid line: shallow array, dashed line: temperature array. Days 216.0 - 216.5.

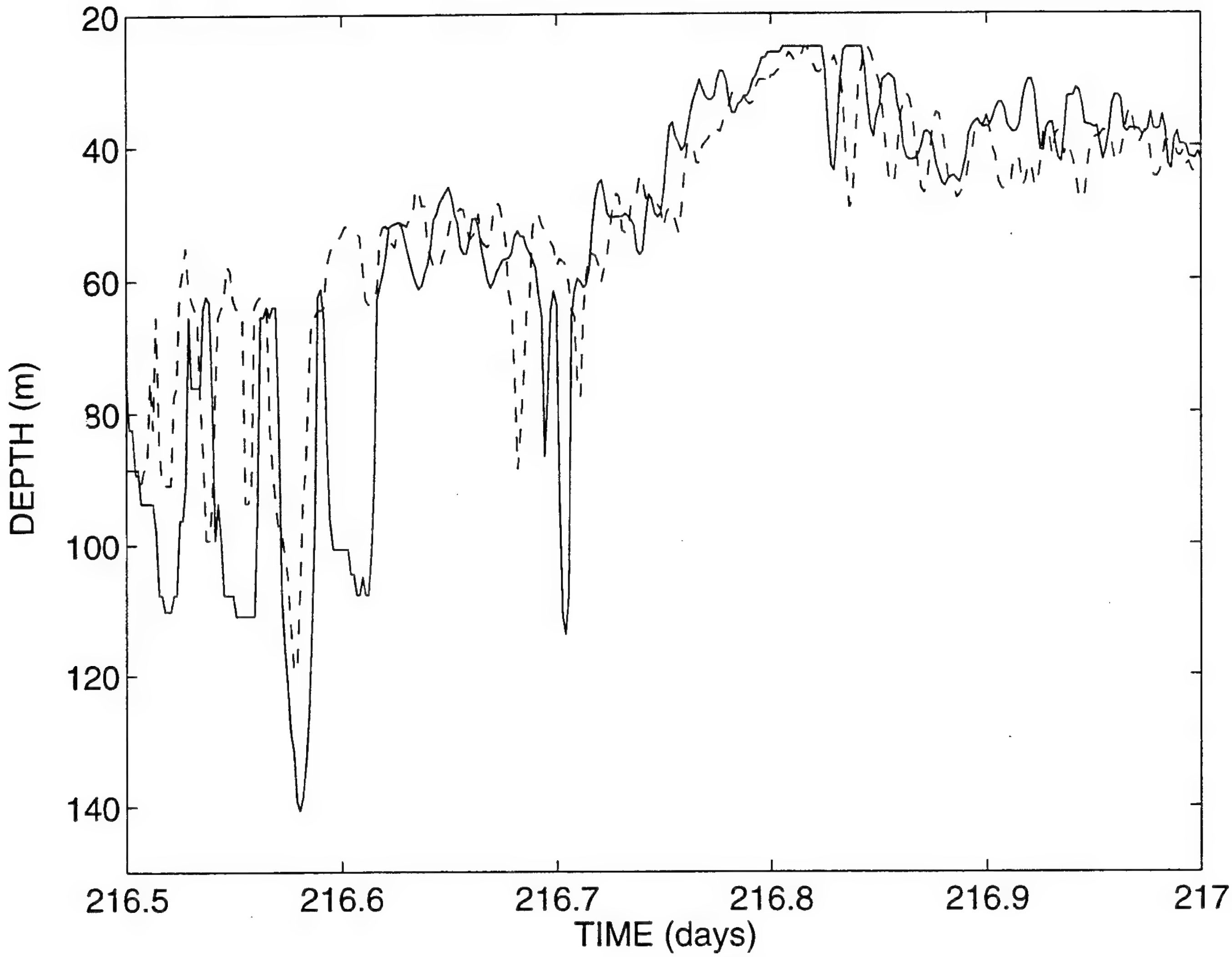


Figure 5(d). Isospeed contours of 1494.5 m/s as functions of depth and time. Solid line: shallow array, dashed line: temperature array. Days 216.5 - 217.0.

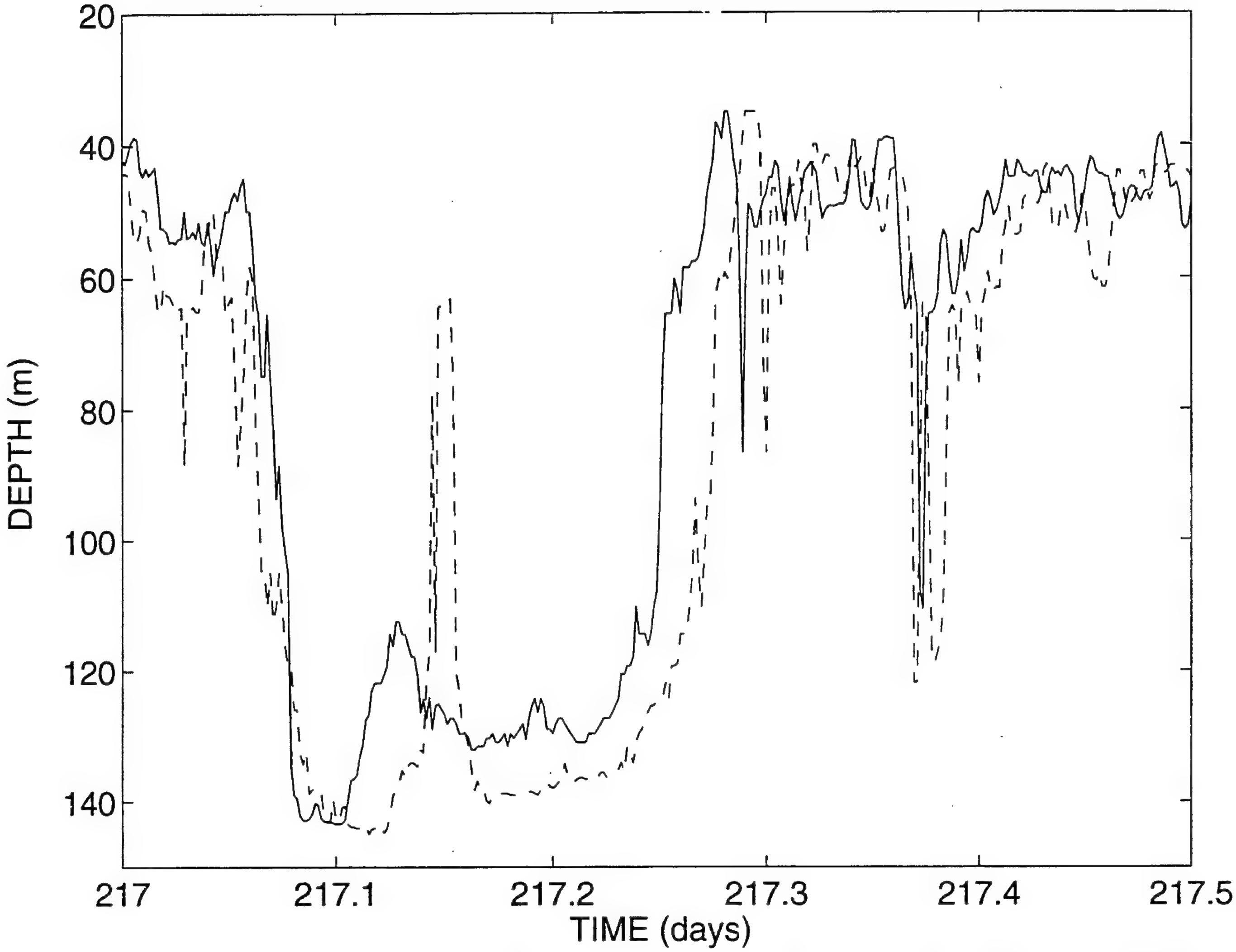


Figure 5(e). Isospeed contours of 1494.5 m/s as functions of depth and time. Solid line: shallow array, dashed line: temperature array. Days 217.0 - 217.5.

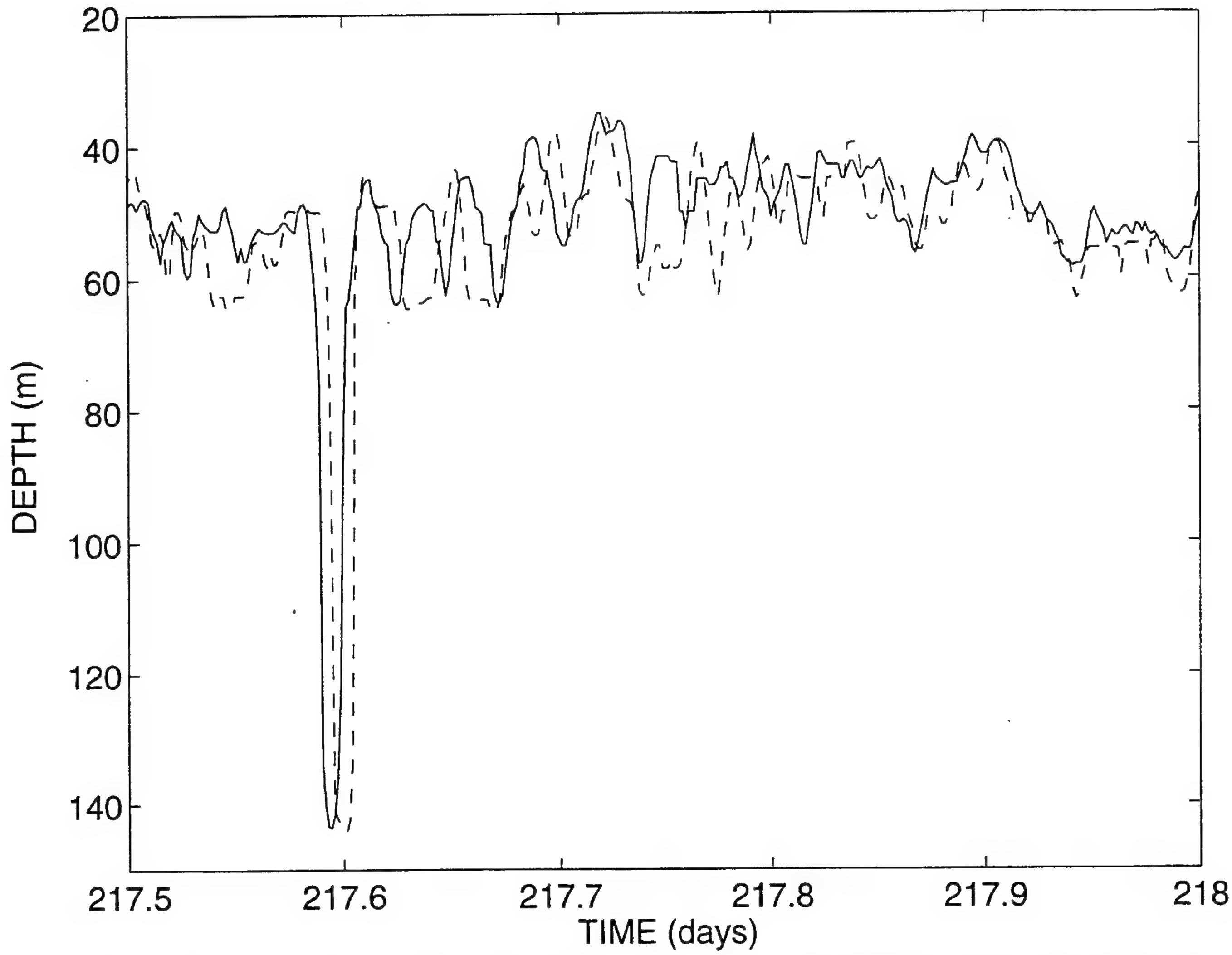


Figure 5(f). Isospeed contours of 1494.5 m/s as functions of depth and time. Solid line: shallow array, dashed line: temperature array. Days 217.5 - 218.0.

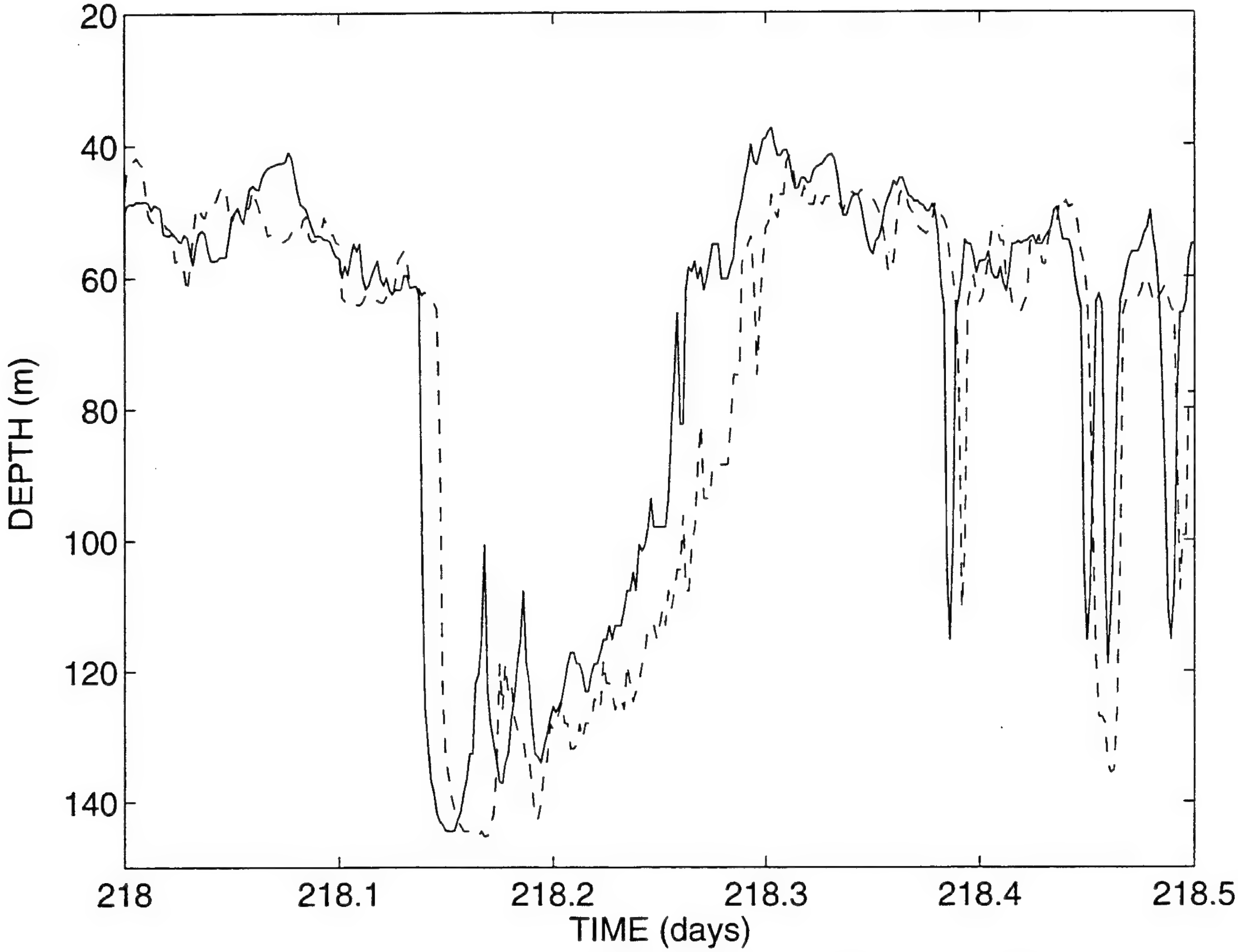


Figure 5(g). Isospeed contours of 1494.5 m/s as functions of depth and time. Solid line: shallow array, dashed line: temperature array. Days 218.0 - 218.5.

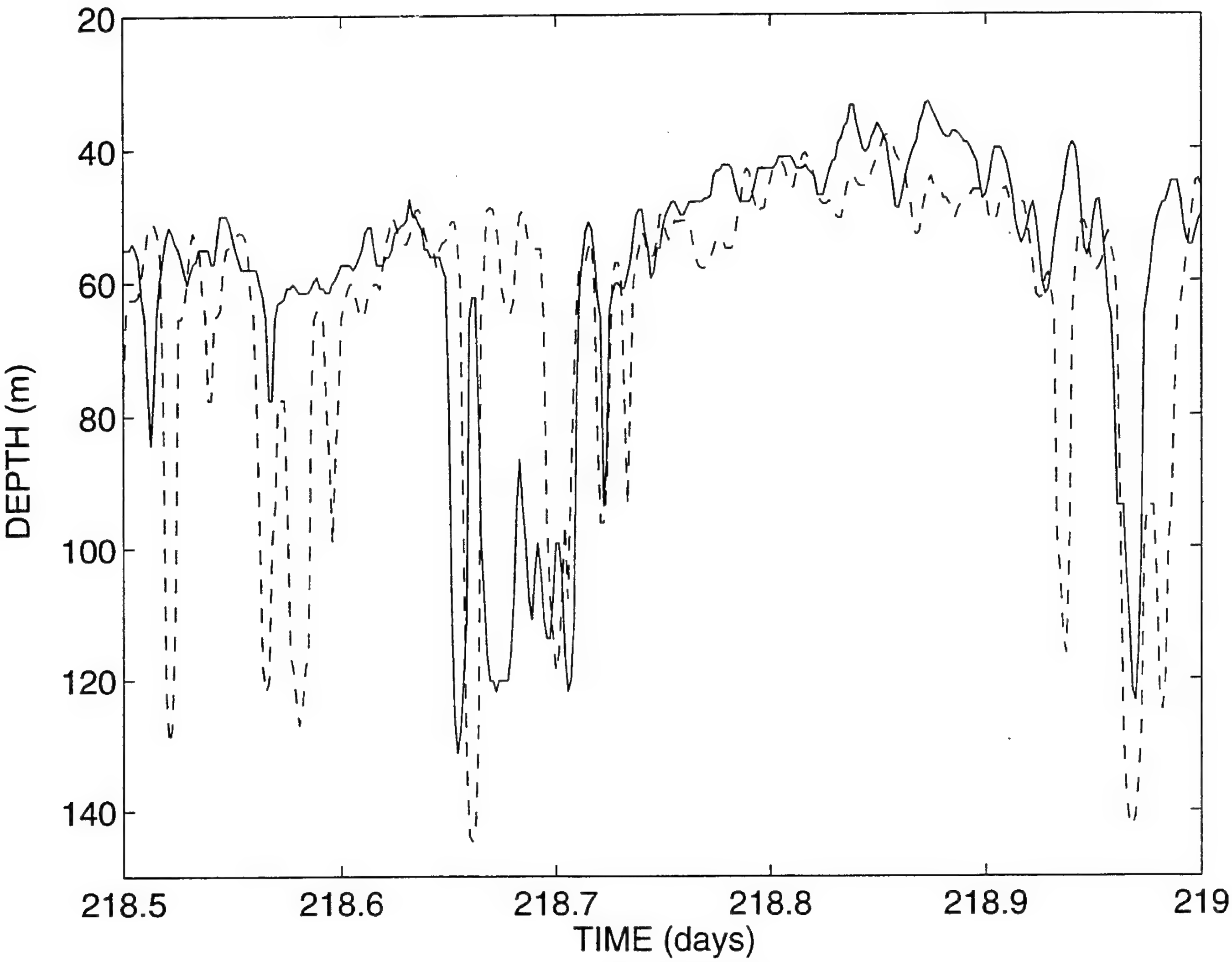


Figure 5(h). Isospeed contours of 1494.5 m/s as functions of depth and time. Solid line: shallow array, dashed line: temperature array. Days 218.5 - 219.0.

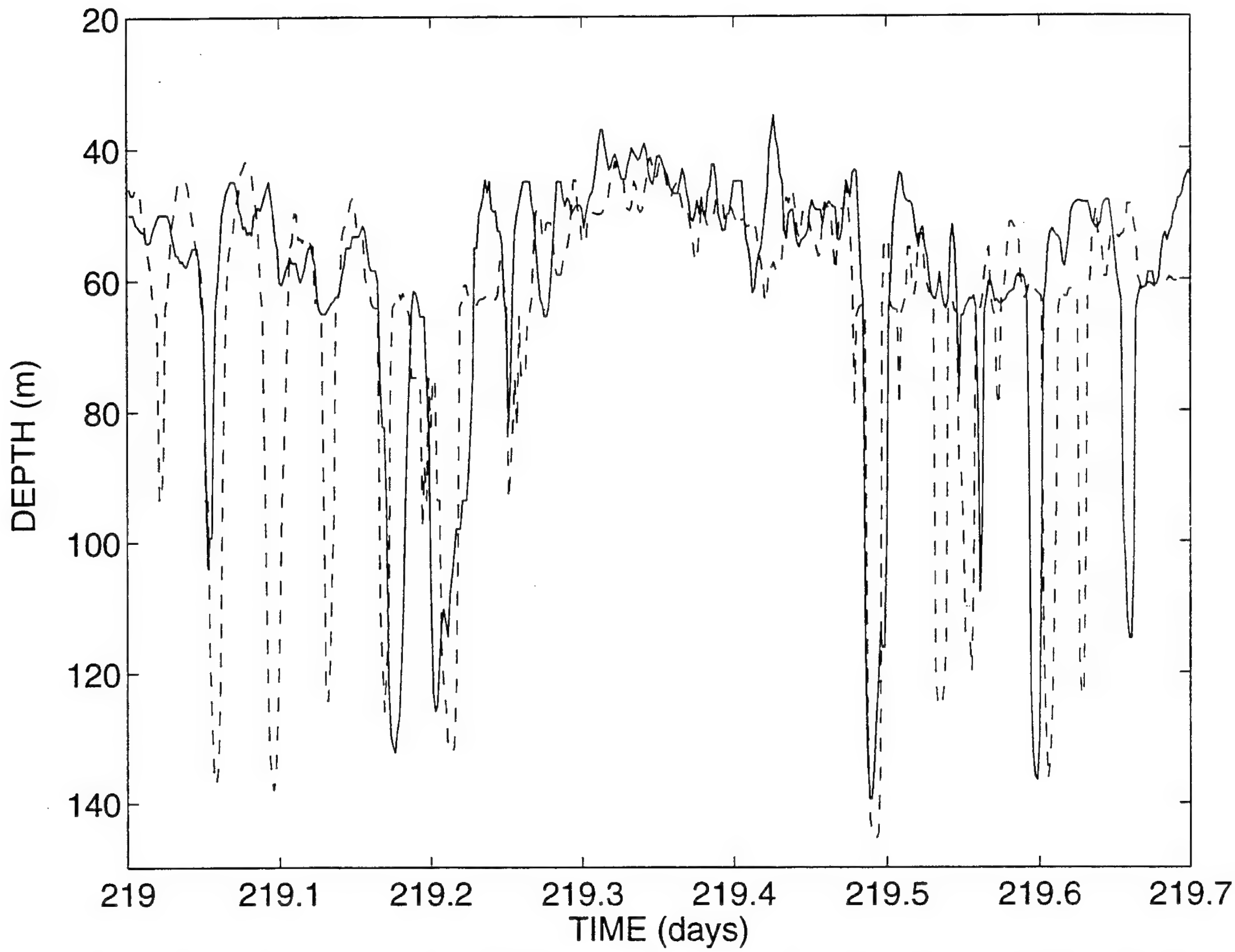


Figure 5(i). Isospeed contours of 1494.5 m/s as functions of depth and time. Solid line: shallow array, dashed line: temperature array. Days 219.0 - 219.7.

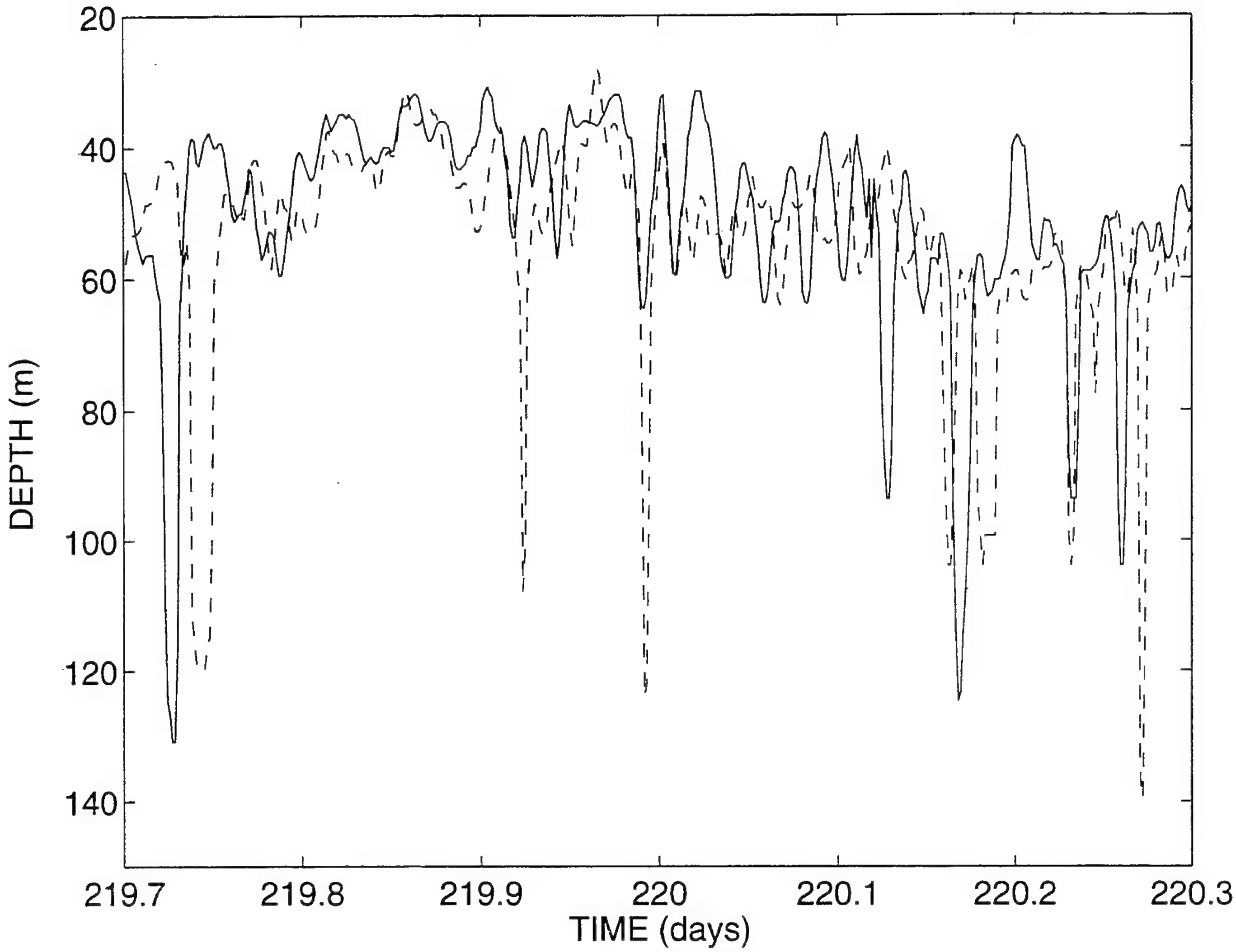


Figure 5(j). Isospeed contours of 1494.5 m/s as functions of depth and time. Solid line: shallow array, dashed line: temperature array. Days 219.7 - 220.3.

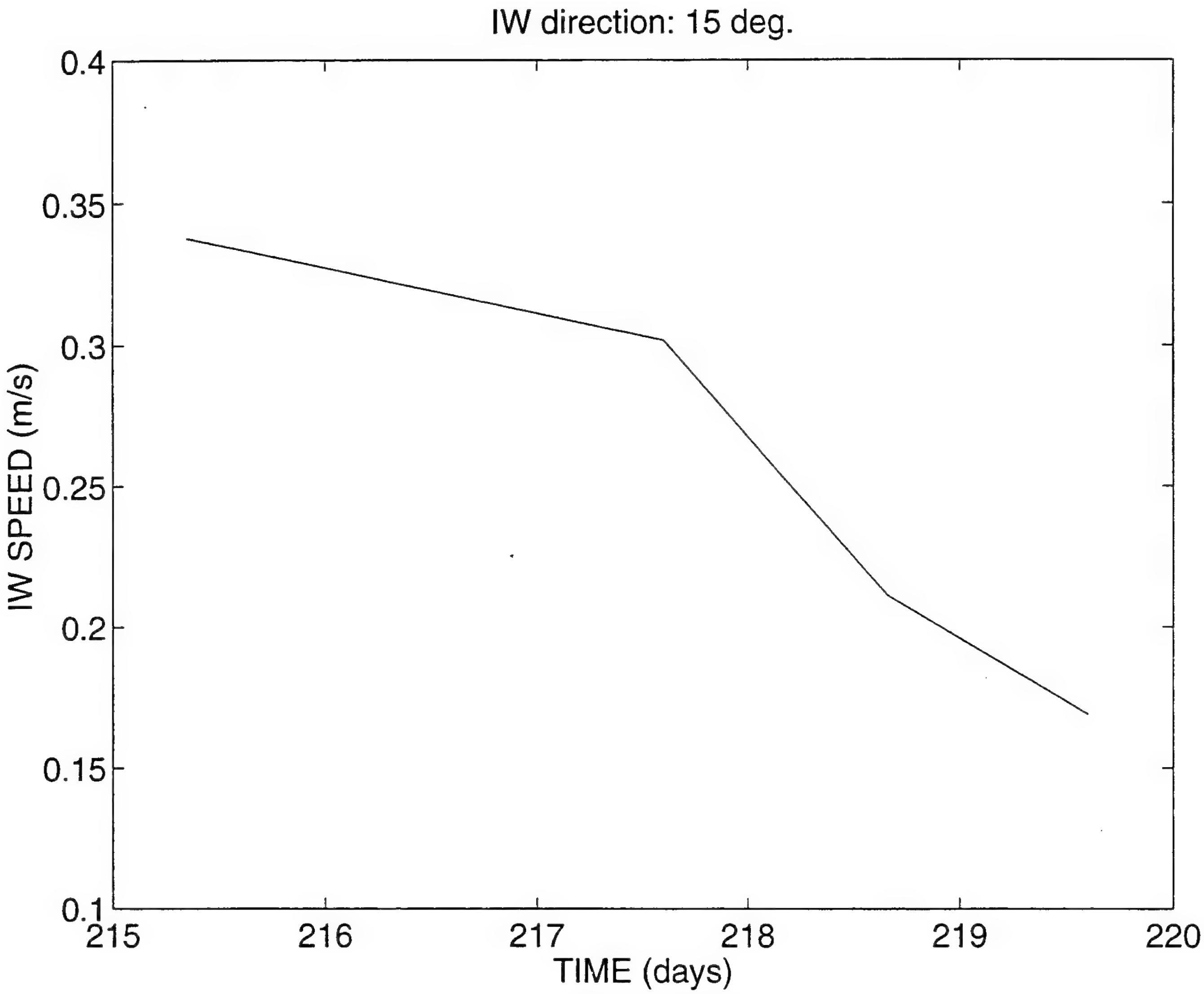


Figure 6. Variations of IW speeds, assuming incident direction for IWs to be $\theta = 15^o$ [angle $\theta$ in Fig. 1 and Eq. (1)].

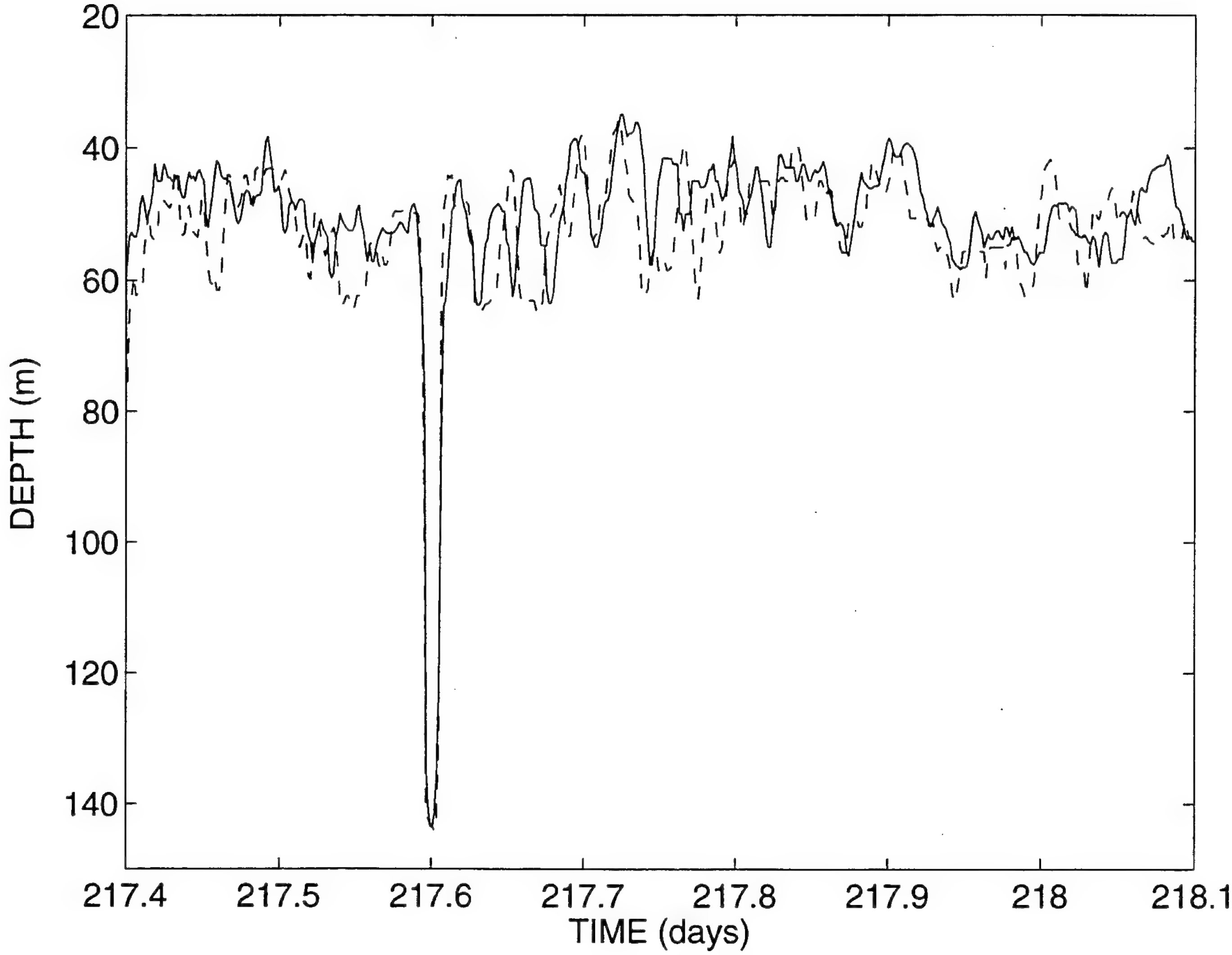


Figure 7. Isospeed contours of 1494.5 m/s as functions of depth and time. Solid line: shallow array, dashed line: temperature array. Days 217.4 - 218.1. The solid line contour (shallow array) has been shifted to the right by 4 samples (time span of 0.0056 days = 8.064 min).

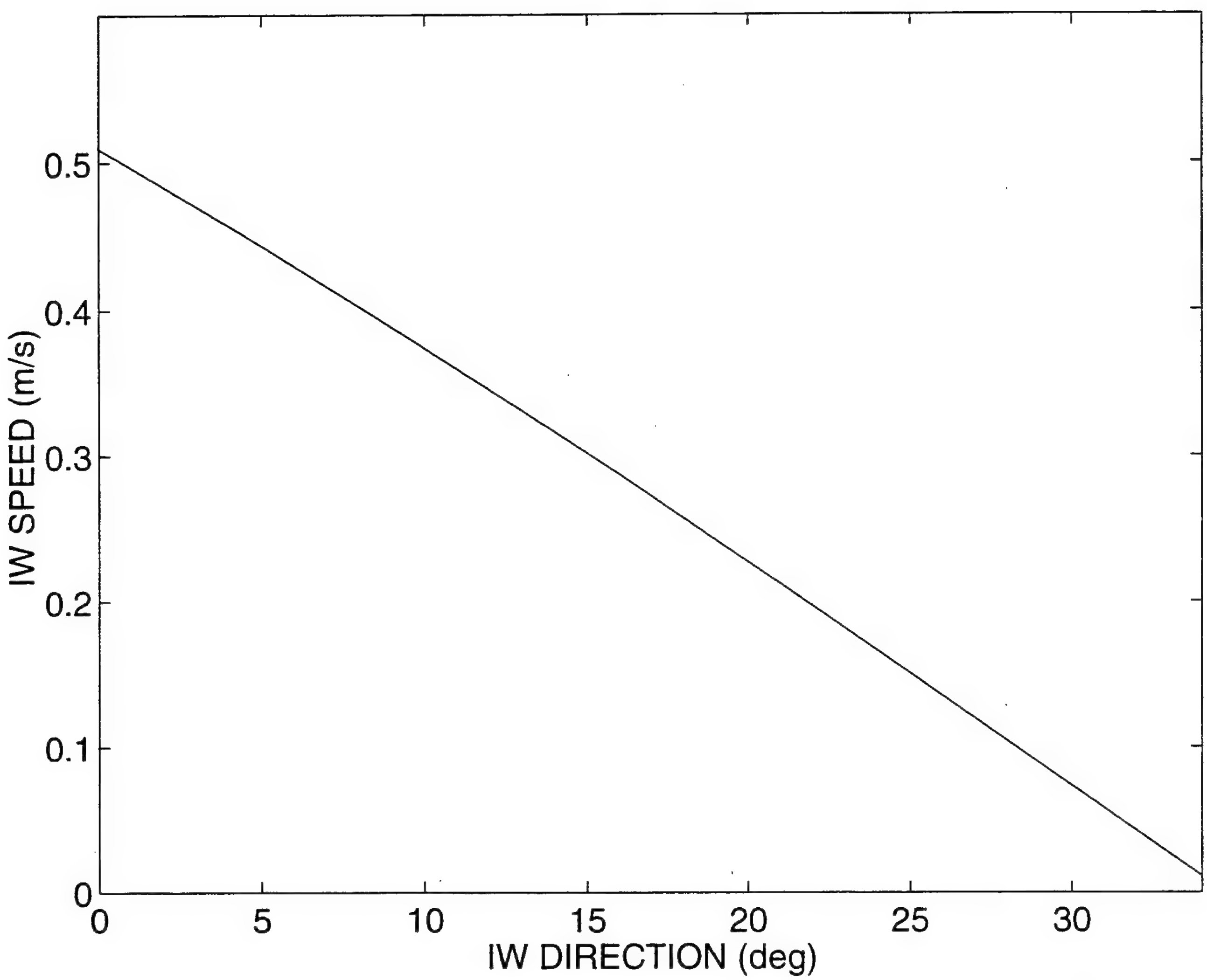


Figure 8. The relation between internal wave speed and its direction [angle θ in Fig. 1 and Eq. (1)].

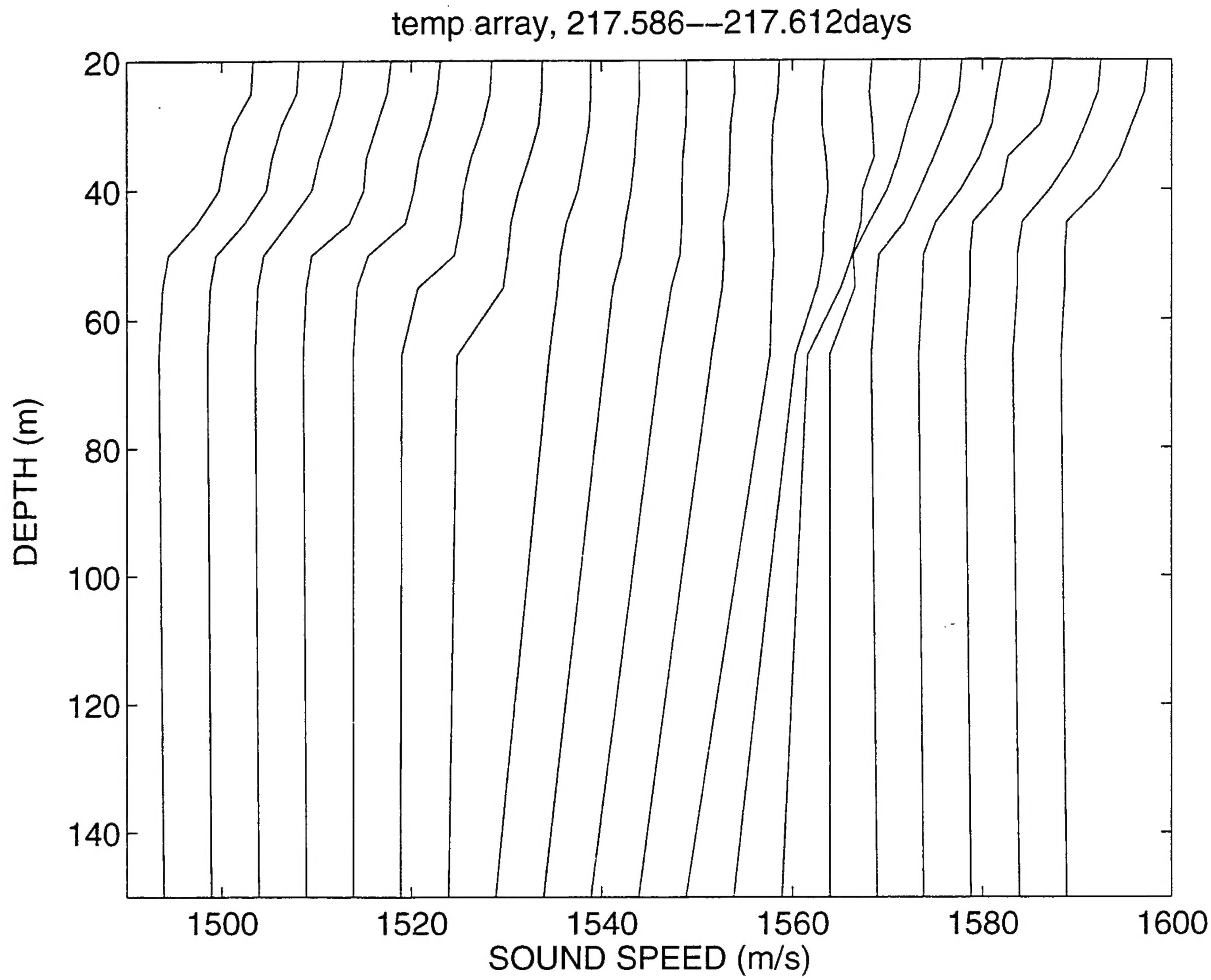


Figure 9(a). Evolution of sound speed profiles during the period days 217.586 - 217.612. Successive sound speed profiles have been shifted by 5 m/s.

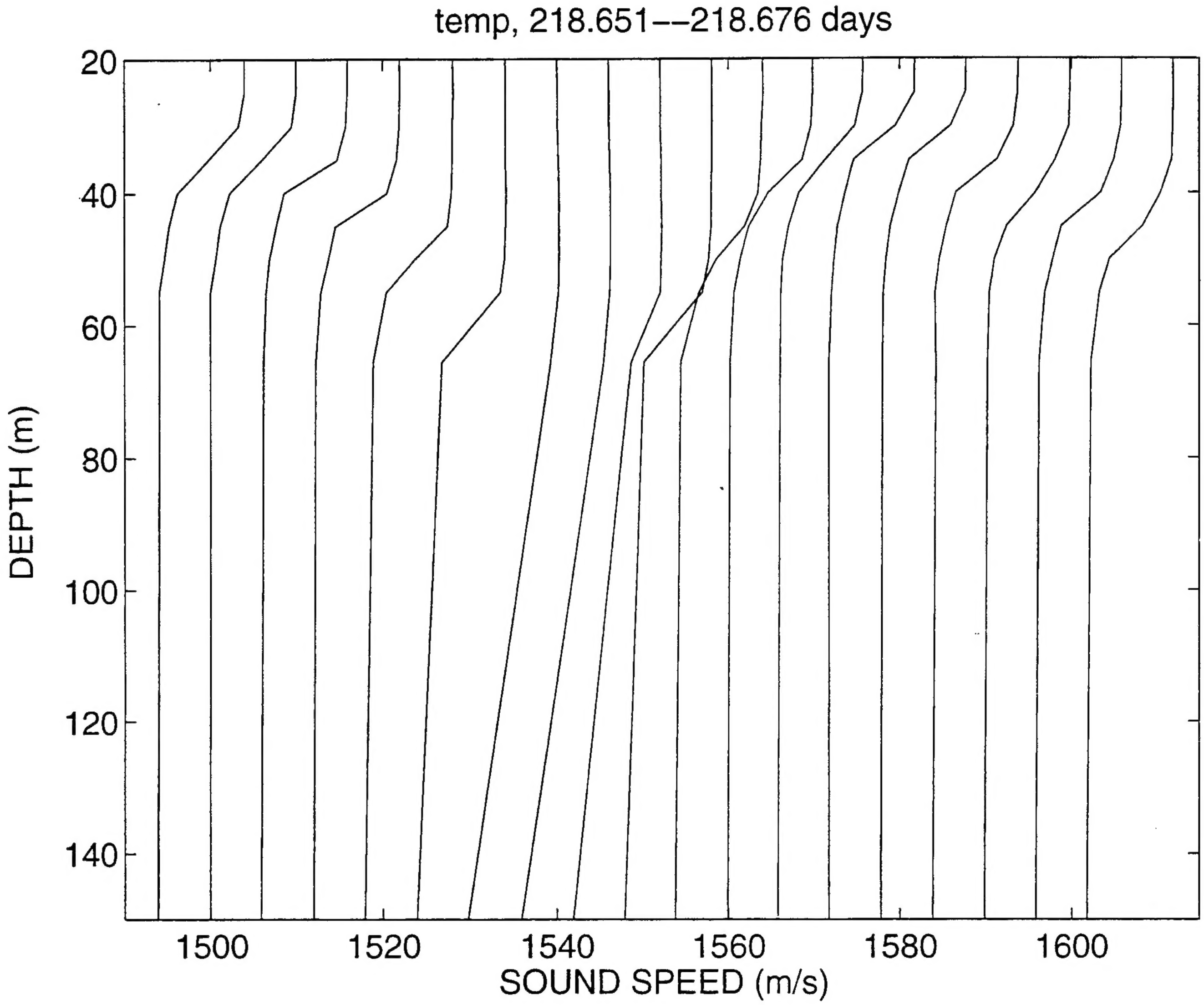


Figure 9(b). Evolution of sound speed profiles during the period days 218.651 - 218.676. Successive sound speed profiles have been shifted by 6 m/s.

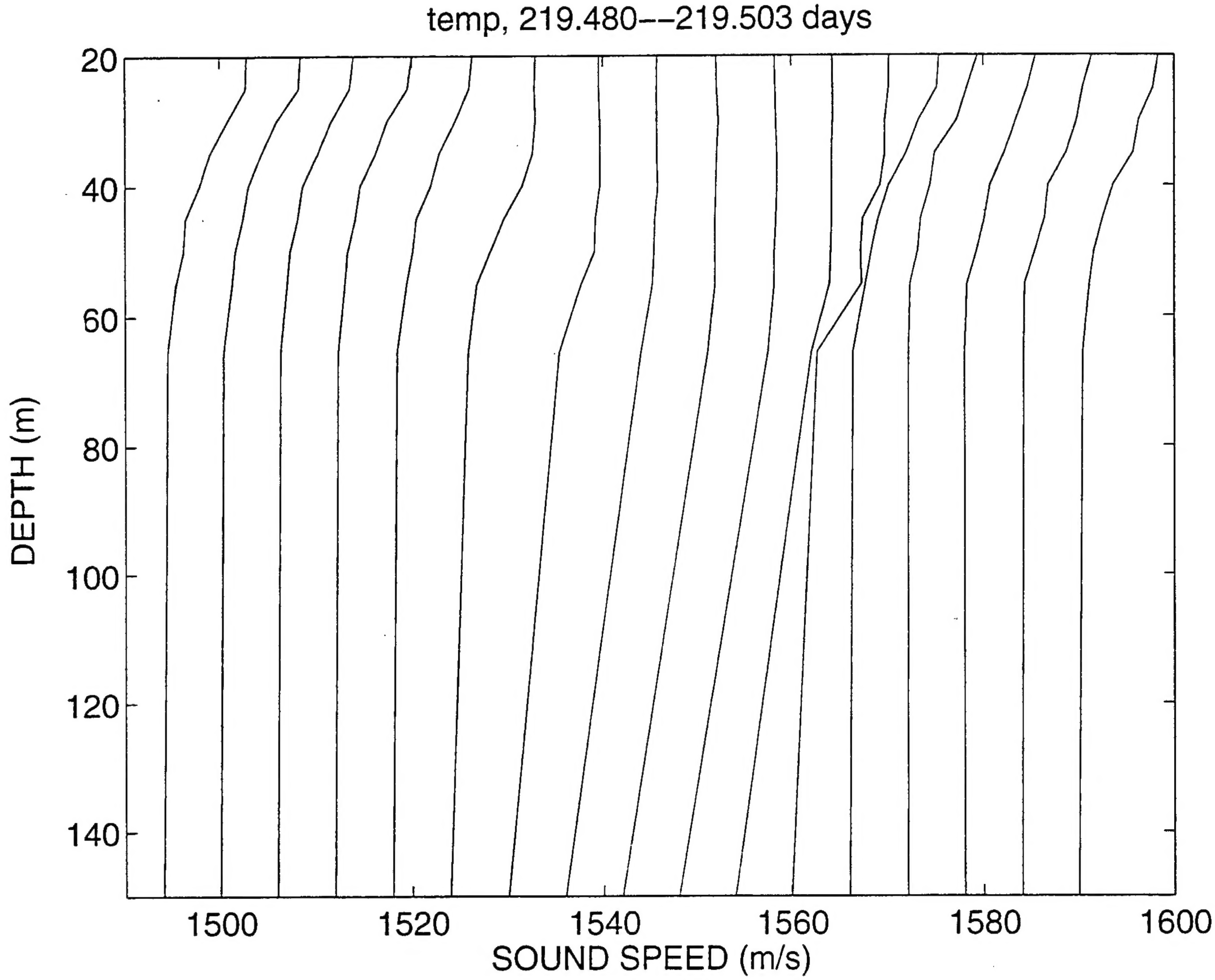


Figure 9(c). Evolution of sound speed profiles during the period days 219.480 - 219.503. Successive sound speed profiles have been shifted by 6 m/s.

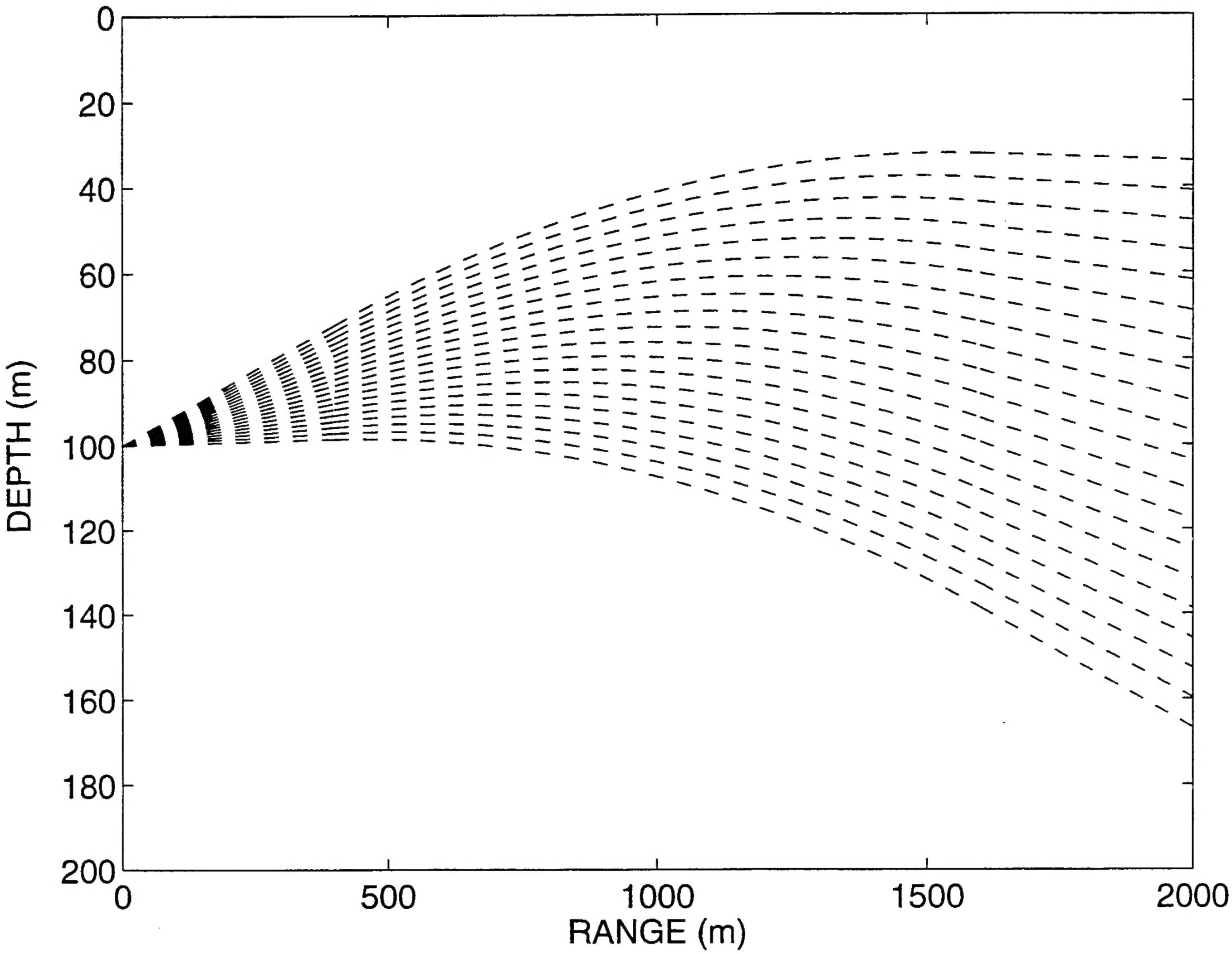


Figure 10. Illustration of ray propagation in 3 regions. Range 0 - 400 m: isospeed region. Range 400 - 1600 m: region with the constant sound speed gradient from the middle period of Fig. 9(a), which has a 16.3 km radius for the circular ray arc. Range 1600 - 2000 m: isospeed region.